Photodegradation of 4″-(Epimethylamino)-4″-deoxyavermectin B_{1a} Thin Films on Glass

William F. Feely,*,† Louis S. Crouch,† Byron H. Arison,‡ William J. A. VandenHeuvel,‡ Lawrence F. Colwell,§ and Peter G. Wislocki†

Department of Animal and Exploratory Drug Metabolism, Pesticide Metabolism and Environmental Safety Group, Merck Sharp and Dohme Research Laboratories, P.O. Box 450, Three Bridges, New Jersey 08887, and Department of Animal and Exploratory Drug Metabolism and Department of Natural Products Chemistry, Merck Sharp and Dohme Research Laboratories, P.O. Box 2000, Rahway, New Jersey 07065

Photodegradation of 4″-(epimethylamino)-4″-deoxyavermectin B_{1a} as thin films on glass, using artificial light, resulted in the formation of multiple photodegradates. Six primary degradates and two secondary degradates were identified. The primary degradates formed were 8,9-*Z*-4″-(epimethylamino)-4″-deoxyavermectin B_{1a} (a geometric isomer), delta 2,3-4″-(epimethylamino)-4″-deoxyavermectin B_{1a} (a positional isomer), avermectin B_{1a} monosaccharide, 4″-epiamino-4″-deoxyavermectin B_{1a}, 4″-*N*-formyl-4″-deoxyavermectin B_{1a}, and 4″-*N*-methyl-*N*-formyl-4″-deoxyavermectin B_{1a}. The secondary degradates formed, both geometric isomers of two primary degradates, were 8,9-*Z*-4″-epiamino-4″-deoxyavermectin B_{1a} and 8,9-*Z*-4″-*N*-formyl-4″-deoxyavermectin B_{1a}. The substitution of the epi-*N*-methylamino group for the hydroxyl group at the 4″ position of avermectin B_{1a} profoundly affected the formation of photodegradates in thin films reported in earlier studies.

INTRODUCTION

The avermectins are new pesticides produced by the actinomycete *Streptomyces avermitilis*. Abamectin, the first-generation commercial product, is currently marketed in the United States and around the world, mainly as a miticide.

An intensive chemical modification and screening program was initiated to discover new avermectins with increased insecticidal activity, especially against lepidopteran larvae (Mrozik et al., 1989). This program resulted in the selection of the semisynthetic derivative, 4″-(epimethylamino)-4″-deoxyavermectin B_{1a} (MAB1a, Figure 1), as a second-generation avermectin pesticide.

Previously, we reported studies of the photodegradation of avermectin B_{1a} (B1a, the main active ingredient of abamectin) as thin films on glass (Crouch et al., 1991). Here we report similar studies with MAB1a. The purpose of these investigations is to characterize and, if possible, identify the photodegradates of MAB1a. Also, since the terminal residues of avermectins on plants are typically in the parts per billion (ppb) range at the normal application rate (approximately 10 g/acre), these thin-film experiments have proven to be useful in generating standards for use in further studies.

MATERIALS AND METHODS

MAB1a and Derivatives. MAB1a, 4″-epiamino-4″-deoxyavermectin B_{1a} (AB1a), 4″-*N*-formyl-4″-deoxyavermectin B_{1a} (FAB1a), and 4″-*N*-methyl-*N*-formyl-4″-deoxyavermectin B_{1a} (MFB1a) were supplied by the Department of Basic Medicinal Chemistry at Merck Sharp and Dohme Research Laboratories. Syntheses of MAB1a and AB1a have been described (Mrozik et al., 1989).

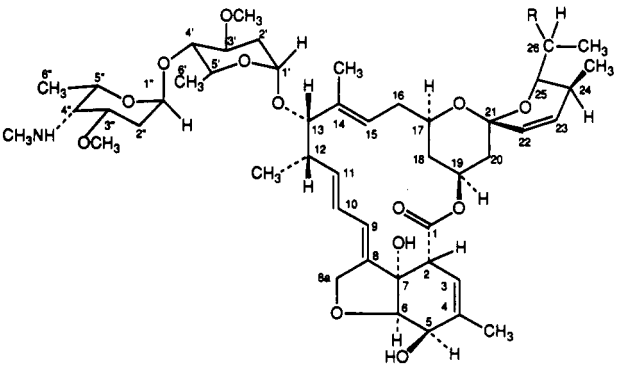

Figure 1. Structure of MAB1a.

Photodegradation of MAB1a Thin Films. MAB1a photodegradation time course studies were performed as with B1a (Crouch et al., 1991). Briefly, aliquots of a methanol solution containing MAB1a were placed on glass Petri dishes at a density of 0.7 $\mu g/mm^2$. The solutions were dried in the dark at room temperature. The thin films were placed 66 cm from a bank of 10–12 General Electric 275W Suntanner RS bulbs in a fume hood. The surface temperature under the lights varied from 40 to 50 °C. Total surface irradiance, measured by a Model 8-48 black and white pyranometer (Eppley Laboratories), was approximately 60–70 mW cm^{-2} h^{-1}.

Thin films of MAB1a were photodegraded for 16 h. Residues were recovered by washing the glass surfaces with methanol (MeOH). All washes were taken to dryness under vacuum and dissolved in an appropriate solvent for HPLC analysis. Samples were purified as described below.

High-Performance Liquid Chromatography (HPLC). All solvents used were of HPLC grade (EM Science). Water was of HPLC grade and was obtained from a Waters Milli-Q water-purifying system. All residues were dissolved in MeOH for reversed-phase (RP) HPLC or mobile phase or ethanol for normal-phase (NP) HPLC. Fractions were obtained either by collection in 7-mL plastic vials with a Pharmacia Fractomette fraction collector or by hand collection of the peak of interest. In all cases, Rheodyne 7125 and 7126 injectors were used to inject samples while Brownlee guard columns, containing either RP or

* Author to whom correspondence should be addressed.
† Department of Animal and Exploratory Drug Metabolism, Three Bridges.
‡ Department of Animal and Exploratory Drug Metabolism, Rahway.
§ Department of Natural Products Chemistry, Rahway.

0021-8561/92/1440-0691$03.00/0 © 1992 American Chemical Society

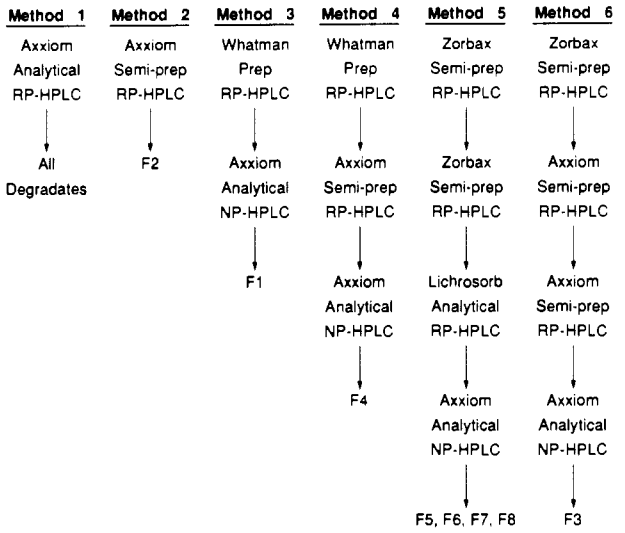

Figure 2. General outline for HPLC methods used to examine and isolate photodegradates of MAB1a.

NP stationary phases, were used to protect the analytical columns. For all degradates, ultraviolet (UV) spectra were obtained with diode array detectors (see below) by scanning the peaks of interest from 200 to 400 or 600 nm.

Due to the wide polarity differences of the products, six different HPLC methods were used to examine and isolate the photodegradates, designated F1–F8, formed from MAB1a. A general outline of the methods (see below) is shown in Figure 2.

Method 1. This method was used to examine the degradates after thin-film photolysis or during purification by other HPLC methods. HPLC was accomplished with a Spectra Physics 8800 ternary pump and an Axxiom Axxi-Chrom ODS analytical column (250 × 4.6 mm) eluted with MeOH/H_2O (v/v) and 5 mM ammonium acetate (for both MeOH and H_2O) at a flow rate of 1 mL/min. A gradient, with the following parameters, was used: 0–45 min, 80–90% MeOH; 45–50 min, increase to 100% MeOH. Residues were monitored by UV detection with a Hewlett-Packard (HP) 1040 M photodiode array detector; the chromatogram was displayed at 245 nm. The detector was linked to an HP Think Jet printer (Model 2225A) and an HP plotter (Model 7475A).

Method 2. HPLC was performed with a Spectra Physics 8800 ternary pump and an Axxiom Axxi-Chrom ODS semipreparative column (250 × 10 mm) eluted with 85/15 MeOH/H_2O and 5 mM ammonium acetate at a flow rate of 4 mL/min. The remaining equipment used was the same as in method 1.

Method 3. HPLC was first performed (step 1) with an LDC Constametric pump and a Whatman Partisil Magnum C_{18} preparative column (500 × 22 mm); the flow was 18 mL/min. The mobile phase consisted of 80/20 MeOH/H_2O containing 10 mM ammonium acetate. UV detection, at 245 nm, was accomplished with an LDC Spectromonitor III equipped with a preparative flow cell attached to an HP integrator (Model 3394A). The second separation (step 2) was accomplished with a Spectra Physics 8700 ternary pump and an Axxiom silica column (250 × 4.6 mm) eluted with 85/15 isooctane/ethanol containing 0.4 mM triethylamine at a flow rate of 2 mL/min. Residues were characterized by UV spectra with an HP 85B diode array detector linked to an HP printer (Model 2225A) and an HP plotter (Model 7475A).

Method 4. The first separation (step 1) was performed as in step 1 of method 3. The second separation (step 2) was performed as above in method 2 except that the mobile phase was changed to 82/18 MeOH/H_2O containing 5 mM ammonium acetate and the flow rate was changed to 3 mL/min. The last separation (step 3) was completed as in step 2 of method 3.

Method 5. The first separation (step 1) was accomplished with a Spectra Physics 8800 ternary pump and a Zorbax ODS semipreparative column (250 × 9.4 mm). The mobile phase consisted of 95/5 MeOH/H_2O and 5 mM ammonium acetate; the flow rate was 3 mL/min. Residues were characterized by UV spectra as above. Samples from this step were then fractionated (step 2) using the same system; however, the mobile phase was changed to 90/10 MeOH/H_2O and 5 mM ammonium acetate. Fractions from the previous step were next purified (step 3) using the same pump and a Lichrosorb ODS column (250 × 4.6 mm) equilibrated with 90/10 MeOH/H_2O and 5 mM ammonium acetate at a flow rate of 1 mL/min. Finally, samples were purified by NP HPLC (step 4). This system consisted of a Spectra Physics 8700 pump connected to an Axxiom silica column (250 × 4.6 mm) eluted with 85/15 isooctane/ethanol and 8 mM triethylamine at a flow rate of 2 mL/min. The chromatogram was monitored at 255 nm with an LDC Spectromonitor detector linked to a Spectra Physics 4200 integrator.

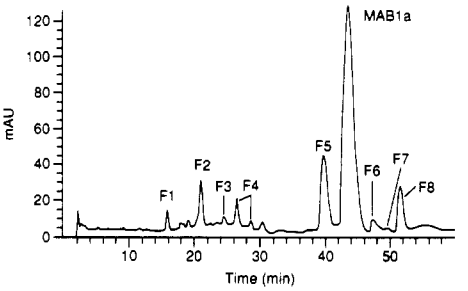

Figure 3. Analytical RP-HPLC (method 1) of photodegradates of MAB1a.

Method 6. The first step (step 1) was completed as in step 1 of method 5. Second (step 2) and third (step 3) separations were carried out as in step 2 of method 4. Finally, the last purification (step 4), NP HPLC, was accomplished as in step 2 of method 3.

Mass Spectrometry and Nuclear Magnetic Resonance Spectroscopy. Fast atom bombardment (FAB) mass spectrometry experiments were performed using a MAT 731 mass spectrometer. Samples were dissolved in lithium acetate/methanol and loaded onto a probe tip coated with a 5:1 solution of dithiothreitol/dithioerythritol ("magic bullet"). Samples were ionized with a xenon gas FAB gun operated at 8 kV; the accelerating voltage also was set at 8 kV. Resolution for these experiments was 1000.

The electron impact (EI) mass spectrometry experiments were done with a MAT 212 mass spectrometer. Samples were placed in a glass crucible and volatilized by applying to the probe tip a linear temperature program, ambient temperature to 300 °C, at a rate of 60 °C/min. The volatilized samples were ionized at 100 eV; the accelerating voltage was set at 3 kV. Resolution for these experiments was also 1000.

Nuclear magnetic resonance spectra were acquired at 400 MHz with a Varian Unity 400 spectrometer. Data were collected at room temperature after the samples were dissolved in $CDCl_3$ using a 1-s acquisition time and a 45° flip angle.

RESULTS

HPLC of Total Residue. A chromatogram (245 nm) of the MAB1a residues that were investigated, after 16 h of photodegradation, is shown in Figure 3. Method 1 was used to resolve the major photodegradates.

Isolation of Photodegradate F2. MAB1a was photolyzed and the residues were chromatographed as stated in method 2 (Figure 4). Photodegradate F2 was isolated from 8 mg of starting material (eight HPLC injections were made); 44 μg of purified photodegradate F2 was obtained.

Isolation of Photodegradate F1. MAB1a (72 mg) was photolyzed and chromatographed as in step 1 of method 3, initially using preparative RP-HPLC (step 1 is shown in Figure 5). One peak (F1) was collected and analyzed by analytical RP-HPLC as in method 1 and appeared relatively pure (data not shown). Photodegradate F1 was isolated by NP-HPLC, using step 2 of method 3, by injecting the sample in two equal portions. Approximately 140 μg of F1 (Figure 6) was obtained.

Isolation of Photodegradate F4. The last fraction of the 72-mg photodegradation mixture from step 1 of method

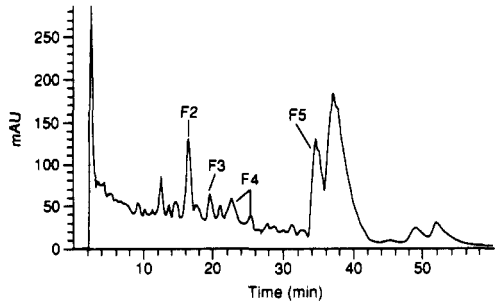

Figure 4. Semipreparative RP-HPLC (method 2) of photodegradates of MAB1a; photodegradate F2 was isolated from this run.

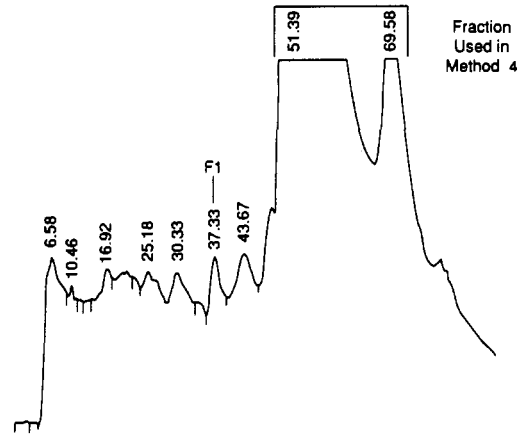

Figure 5. Preparative RP-HPLC (method 3, step 1) of photodegradates of MAB1a; position of photodegradate F1 is designated.

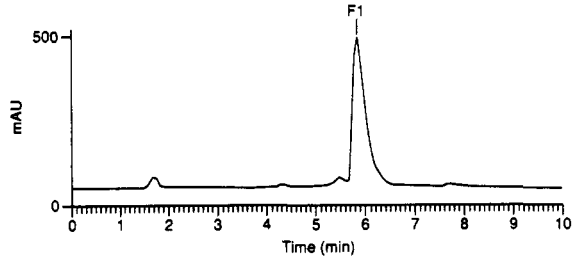

Figure 6. Analytical NP-HPLC (method 3, step 2) of peak F1 from Figure 5; photodegradate F1 was isolated from this run.

3 (Figure 5) was used in step 1 of method 4 to obtain photodegradate F4. This fraction contained mostly MAB1a but also contained the compound of interest, F4 (Figure 3). About half of the fraction was diluted with CH_3CN (9:1 CH_3CN/H_2O v/v) to form an azeotrope, evaporated to dryness, and reconstituted in MeOH. Photodegradate F4 (data not shown; similar to Figure 4) was purified by semipreparative RP-HPLC (18 injections), using step 2 of method 4, and was again taken to dryness as an azeotrope. F4 was always obtained as two peaks, the larger one always eluting before the smaller one in a ratio of about 4:1. This suggested that F4 consisted of interconvertible forms. Finally, about 57 μg of F4 was obtained after NP-HPLC, with step 3 of method 4, by injecting the sample in two equal portions (results not shown).

Isolation of Photodegradates F5–F8. Thirteen milligrams of MAB1a was photolyzed, and the resulting mixture of degradates was initially fractionated, using semipreparative RP-HPLC in step 1 of method 5, by cutting out all the material eluting before photodegradate F5 (data not shown; similar to Figures 3 and 4). F5 and the degradates eluting behind it were taken to dryness as an azeotrope as described above. Most of the MAB1a

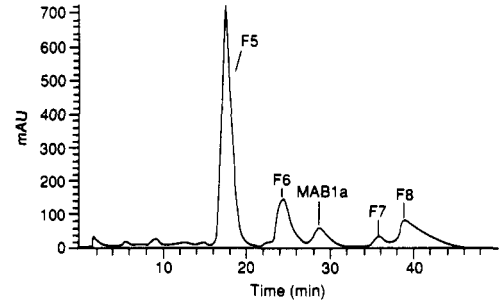

Figure 7. Analytical RP-HPLC (method 5, step 3) of photodegradates of MAB1a; positions of photodegradates F5, F6, F7, and F8 are designated.

Table I. EI and FAB MS Data for MAB1a and Photodegradates Isolated from 16-h MAB1a Thin Films

	EI MS m/z ion for indicated compound						
carbon[a]	MAB1a	F1	F2	F3	F4	F5	F8
1″–5″	158	NP[b]	172	ND[c]	186	144	158
1–26	566	566	566	ND	566	566	566
13–26	305	305	305	ND	305	305	305
FAB MS, mol wt	885	728	899	899	913	871	885

[a] See Figure 1 for carbon numbering scheme. [b] NP, not present. [c] ND, not determined.

was removed from this fraction in step 2 of method 5 (semipreparative RP-HPLC) by injecting one-fifth of the fraction five times (data not shown; similar to Figures 3 and 4). The remainder of the fraction was collected, combined, and separated into MAB1a and peaks F5–F8 by analytical RP-HPLC using step 3 of method 5 (Figure 7; eight injections, fractions taken to dryness as azeotrope). Finally, NP-HPLC (step 4 of method 5, similar to Figure 6) was used to obtain F5 (500 μg), F6 (42 μg), F7 (10 μg), and F8 (140 μg).

Isolation of Photodegradate F3. The first half of the photodegradates separated in step 1 of method 5 were used in step 1 of method 6. The first half was azeotroped as above. Using semipreparative RP-HPLC (step 2 of method 6), photodegradates F1, F2, and F4 were removed (data not shown); the remaining material was combined, taken to dryness as an azeotrope, and dissolved in MeOH. In step 3 of method 6 (semipreparative RP-HPLC) photodegradate F3 was isolated (not shown; similar to Figures 3 and 4), and using NP-HPLC in step 4 of method 6, about 25 μg of F3 was obtained (similar to Figure 6).

After these studies were completed, two Axxiom ODS preparative HPLC columns (25 cm × 21.5 mm each) were linked together and tried as a first separation step for these mixtures. They were superior to the Whatman preparative column and should easily scale down directly to semipreparative and analytical isolation schemes.

Mass Spectrometry and Nuclear Magnetic Resonance Spectroscopy. The EI and FAB MS data for the degradates, isolated according to the procedures outlined above, and for MAB1a are compared and shown in Table I. These values are related to the known EI MS ions for B1a (Albers-Schonberg et al., 1981) and with the EI MS ions and FAB parent ions for B1a and the degradates formed from it (Crouch et al., 1991).

The numbering scheme for avermectin substructures is shown in Figure 1. MAB1a and the photodegradates formed from it possess intact macrocycles; EI MS ions of m/z 566, indicative of carbon atoms 1–26, and ions of m/z 305, indicative of carbon atoms 13–26, are present in all isolates (Table I). Photodegradate F1 has lost the outer oleandrose sugar; its molecular weight (MW), determined

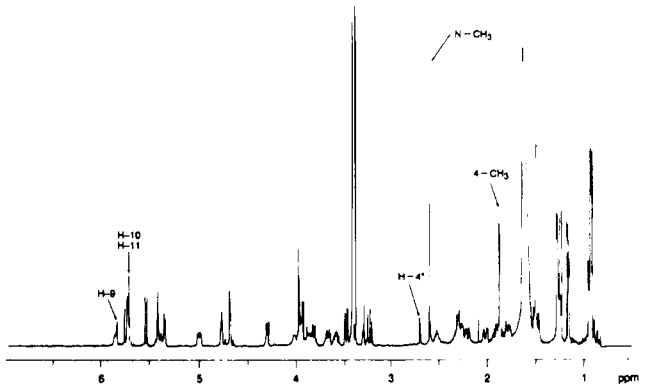

Figure 8. Proton NMR of MAB1a at 400 MHz.

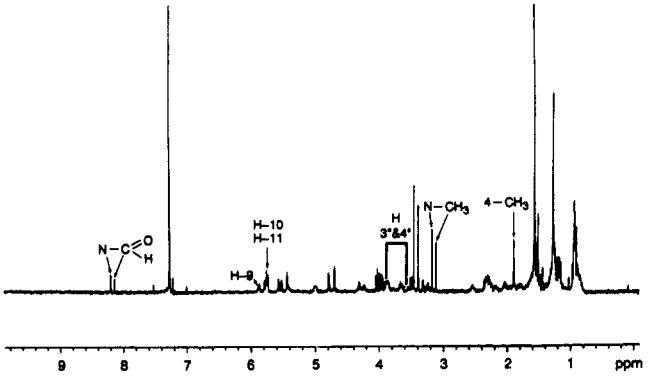

Figure 9. Proton NMR of F4 (MFB1a) at 400 MHz.

by FAB MS, is 728 vs 885 for MAB1a. Therefore, F1 was identified as the monosaccharide of MAB1a (MSB1a). Photodegradates F2 and F3 result from an increase of 14 mass units to the parent structure; the MW of F2 and F3 is 899 vs 885 for MAB1a (Table I). In addition, for F2, the increase in mass occurs on the outer sugar as determined by EI MS; for C1″–C5″ the m/z ion of F2 is 172 vs 158 for MAB1a. Photodegradate F4 results from an increase of 28 mass units to the outer sugar (m/z ion of 186 vs 158 for MAB1a from EI MS). Photodegradate F5 has lost 14 mass units on the terminal oleandrose sugar, m/z ion of 144 vs 158 for MAB1a. Photodegradates F6 and F7 were not examined by MS. Finally, the MS of photodegradate F8 was unchanged compared to that of MAB1a.

The proton NMR spectrum of MAB1a is shown in Figure 8. Prominent features include the *N*-methyl peak at 2.6 ppm, H-10 and H-11 signals between 5.7 and 5.8 ppm, H-9 peaks between 5.8 and 5.9 ppm, and a 4-methyl signal at 1.87 ppm. F1 was not examined by NMR. F2 is distinguished by the lack of an *N*-methyl peak and a slightly broadened singlet at 8.38 ppm (data not shown); with the MS data, this degradate was identified as the formamide of MAB1a (FAB1a). F3 was not studied by NMR. The NMR spectrum of F4 is shown in Figure 9; it possesses two peaks at 8.15 ppm. The presence of two closely related species was evident from the doubling of a number of signals associated with protons on the outer sugar. The single *N*-methyl peak has shifted downfield and appears as two peaks centered at 3.14 ppm. These and the MS data suggest F4 is *N*-formyl-MAB1a (MFB1a, cis and trans rotamers). Photodegradate F5 also lacked an *N*-methyl peak by NMR, and a broadened singlet at 3.04 ppm was assigned to H-4″ (data not shown, refer to Figure 8). On the basis of NMR and MS information, this compound was identified as the *N*-demethyl derivative of MAB1a (AB1a). By NMR, F6 resembled F5 except that the H-10

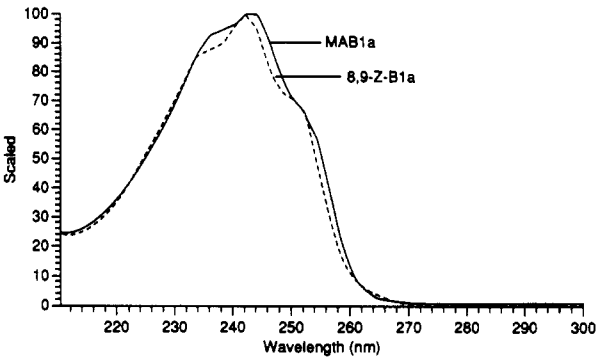

Figure 10. Diode array spectra of MAB1a and 8,9-*Z*-B1a.

signal was shifted downfield to 6.45 ppm (not shown), indicative of the 8,9-*Z* analogues (MAB1a has the 8,9-*E* configuration) of avermectins previously described (Mrozik et al., 1988; Crouch et al., 1991). For F7, the absence of a typical 4-methyl signal near 1.90 ppm coupled with the presence of a singlet at 6.15 ppm (1 H), assigned to a deshielded H-3, strongly suggested that F7 was the delta 2,3-isomer of MAB1a (the double bond at C-3,4 has shifted to C-2,3); the *N*-methyl and H-4″ signals were unaffected. Lastly, photodegradate F8 also possessed the low-field H-10 signal at 6.45 ppm, and since the MS indicated the same molecular weight as MAB1a, this degradate was described as 8,9-*Z*-MAB1a.

HPLC with Standards and Ultraviolet (UV) Spectroscopy. Photodegradates F2, F4, and F5 coeluted with standard FAB1a, MFB1a, and AB1a, respectively, using analytical RP-HPLC (method 1). When these peaks were collected individually from the RP-HPLC experiments, taken to dryness, reconstituted in solvent, and further examined by NP-HPLC (e.g., method 3, step 2), coelution with standards was still observed (data not shown).

Photodegradates F1, F2, F4, and F5 all displayed the same UV spectrum as MAB1a (Figure 10) when examined by photodiode array detection. MAB1a possesses essentially the same UV spectrum as B1a (Crouch et al., 1991). In addition, F3, F6, and F8 have UV spectra identical to the geometric isomer of B1a, 8,9-*Z*-B1a, (Figures 10 and 11; Crouch et al., 1991) formed in thin films. Finally, when FAB1a and AB1a were separately photodegraded as thin films, the first degradates formed were, respectively, F3 and F6 (not shown) as determined by HPLC retention time and UV spectra. Therefore, since F3 has the same molecular weight as F2 and since F3 possesses the UV spectrum of an 8,9-*Z* analogue, F3 was identified as 8,9-*Z*-FAB1a. Similarly, since F6 has the same NMR spectrum as F5 (except for the downfield shift of the H-10 signal) and since F5 possesses the UV spectrum of an 8,9-*Z* analogue, F5 was identified as 8,9-*Z*-AB1a.

DISCUSSION

The designations and abbreviations used for MAB1a photodegradates are summarized in Table II, and the structures of these compounds are shown in Figure 11. Of the eight photodegradates found in these studies, six involve changes to the outer oleandrose sugar (F2–F6 and F8). Also, two degradates (F3 and F6) have two changes in structure, involving the diene and the outer sugar, compared to MAB1a.

MSB1a (F1) has been described previously as an acid hydrolysis product (Fisher and Mrozik, 1989) of B1a. In thin films it is probably formed by simple cleavage of the ether linkage, between the two sugar moieties, to a free radical which reacts to form MSB1a.

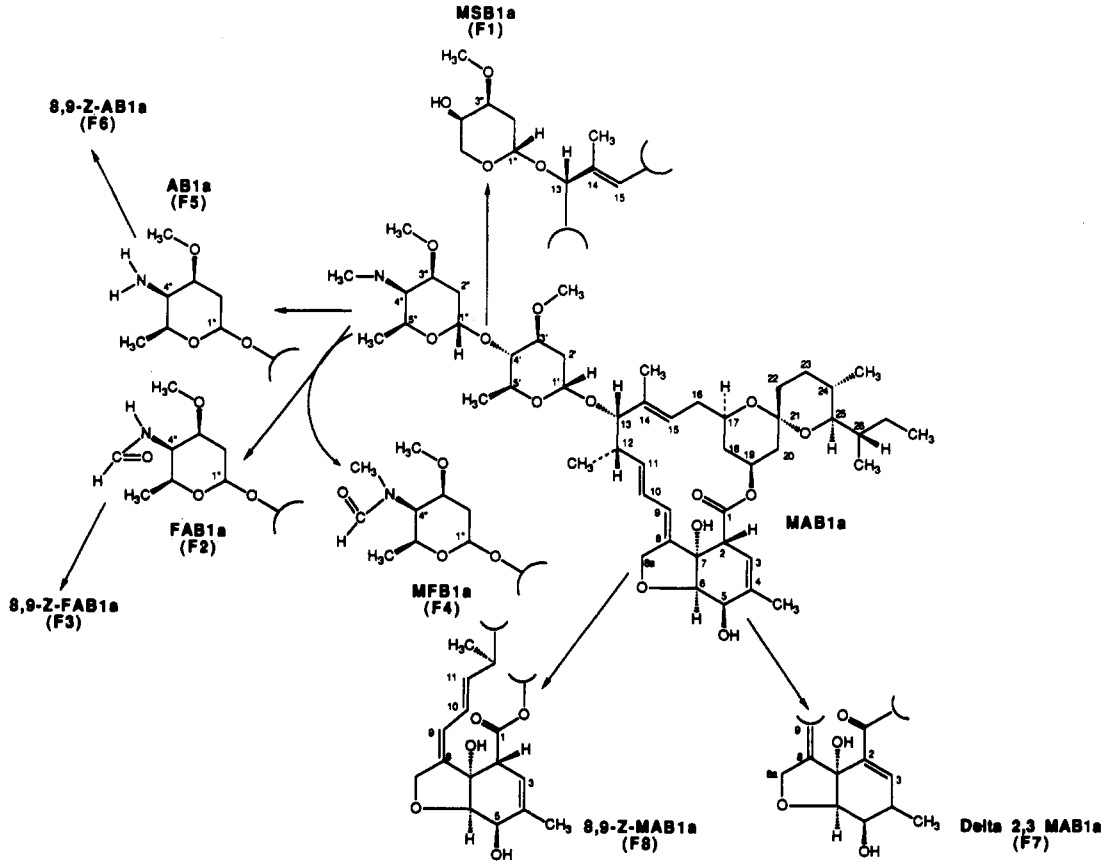

Figure 11. Photodegradates of MAB1a.

Table II. Designations and Abbreviations Used for Photodegradates Generated from 16-h MAB1a Thin Films

F1, MSB1a	F4, MFB1a	F7, delta 2,3-MAB1a
F2, FAB1a	F5, AB1a	F8, 8,9-*Z*-MAB1a
F3, 8,9-*Z*-FAB1a	F6, 8,9-*Z*-AB1a	

In a B1a thin-film photolysis study, Crouch et al. (1991) suggested that singlet oxygen was involved in the formation of some of the photodegradates of B1a. Amines are known quenchers of singlet oxygen, and during quenching, reaction with singlet oxygen can occur (Monroe, 1977). Oxidation to *N*-formyl groups (Fisch et al., 1971) and N-demethylation (Linder et al., 1972) have been described as photooxidative reactions involving amines and singlet oxygen. Therefore, FAB1a (F2) and AB1a (F5) could be formed in the same way.

The 8,9-*Z* isomer of B1a has been reported as a photoproduct of B1a in solution (Mrozik et al., 1988), in thin films (Crouch et al., 1991), and on plants (Maynard and Maynard, 1989; Moye et al., 1990). Similarly, 8,9-*Z*-FAB1a (F3), 8,9-*Z*-AB1a (F6), and 8,9-*Z*-MAB1a (F8) are formed during exposure of MAB1a thin films to light.

Formation of the delta 2,3-epimer of B1a by treatment with base has been described (Pivnichny et al., 1983, 1988). How delta 2,3-MAB1a (F7) is formed in thin films is unknown.

MFB1a (F4) could be formed by addition of a formyl group to MAB1a or addition of a methyl group to FAB1a; in either case this appears to be a unique reaction. An experiment in which the *N*-methyl group of MAB1a is labeled with deuterium, carbon-13, or carbon-14 would help to establish the source of the added group.

In the B1a thin-film study completed by Crouch et al. (1991) the C-14,15 double bond was the region most sensitive to photodegradation; alterations to the macrolide ring also occurred at C-8a. In the present MAB1a thin-film study none of these degradates were detected; the region most sensitive to photodegradation was the *N*-methyl group.

In the B1a study, two geometric isomers, 8,9-*Z*-B1a and 10,11-*Z*-B1a, were formed as well as 3″-*O*-demethyl-B1a. In the MAB1a study, 8,9-*Z*-MAB1a was formed but no 10,11-*Z* isomer was detected and no alterations were seen at C-3″, possibly because of steric hindrance caused by the addition of the *N*-methyl group at C-4″ in MAB1a. In addition, no 10,11-*Z* isomer of MAB1a was observed when MAB1a was photolyzed in solution under anaerobic conditions using simulated sunlight (Crouch et al., unpublished data).

In the B1a thin-film study, only primary degradates were found; no secondary degradates similar to F3 or F6, generated from MAB1a, are formed. The half-life of MAB1a (6.2 h) was longer than the half-life of B1a (2.4 h) under the stated conditions. Clearly, most of the differences mentioned above result from the substitution of the epi-*N*-methylamino group for the hydroxyl group at the 4″ position.

Extended photolysis of MAB1a (little or no parent remaining) results in polar residues as evidenced by lack of retention on reversed-phase HPLC (data not shown). Polar residues were also observed after extended photolysis of B1a (Crouch et al., 1991). Little information concerning the identity of these polar residues has been obtained. Since all diene UV absorbance is eventually lost during photodegradation of MAB1a and B1a, the diene must undergo reactions other than *E,Z* isomerizations. It is possible that singlet oxygen could be involved in photooxidation of the diene in avermectins. Dienes undergo a Diels–Alder-like reaction with singlet oxygen acting as dienophile (Foote and Wexler, 1964). Experiments with singlet oxygen generating systems could

establish the role, if any, of singlet oxygen in photodegradation of these compounds.

The present studies have shown that the substitution of an *N*-methylamino group for the hydroxyl group of avermectin B_{1a} profoundly affects the formation of photodegradates in thin films. Future photodegradation studies with MAB1a degradates and with homologues of MAB1a are planned. Investigations are currently in progress to identify the residues of MAB1a that are formed on plants during normal field practices. These studies should shed new light on the processes involved in thin-film avermectin photochemistry and allow investigators to conduct further studies with new knowledge of the potential products.

ACKNOWLEDGMENT

We thank J. L. Smith for advice and assistance with the MS experiments.

LITERATURE CITED

Albers-Schonberg, G.; Arison, B. H.; Chabala, J. C.; Douglas, A. W.; Eskola, P.; Fisher, M. H.; Lusi, A.; Mrozik, H.; Smith, J. L.; Tolman, R. L. Avermectins: Structure Determination. *J. Am. Chem. Soc.* **1981**, *103*, 4216.

Crouch, L. S.; Feely, W. F.; Arison, B. H.; VandenHeuvel, W. J. A.; Colwell, L. F.; Stearns, R. A.; Kline, W. F.; Wislocki, P. G. Photodegradation of Avermectin B_{1a} Thin Films on Glass. *J. Agric. Food Chem.* **1991**, *39*, 1310.

Fisch, M. H.; Gramain, J. C.; Olesen, J. A. Photo-oxidation of Amines: a Reply. *Chem. Commun.* **1971**, 663.

Fisher, M. H.; Mrozik, H. Chemistry. In *Ivermectin and Abamectin*; Campbell, W. C., Ed.; Springer-Verlag: New York, 1989.

Foote, C. S.; Wexler, S. Olefin Oxidations with Excited Singlet Molecular Oxygen. *J. Am. Chem. Soc.* **1964**, *86*, 3879.

Linder, J. H. E.; Kuhn, H. J.; Gollnick, K. *Tetrahedron Lett.* **1972**, *17*, 1705.

Maynard, M.; Maynard, H. HPLC Assay for Avermectin B_{1a} and its Two Photoisomers Using a Photo Diode Array Detector. *Bull. Environ. Contam. Toxicol.* **1989**, *43*, 499.

Monroe, B. M. Quenching of Singlet Oxygen by Aliphatic Amines. *J. Phys. Chem.* **1977**, *81*, 1861.

Moye, H. A.; Malagodi, M. H.; Yoh, J.; Deyrup, C. L.; Chang, S. M.; Leibee, G. L.; Ku, C. C.; Wislocki, P. G. Avermectin B_{1a} metabolism in Celery: A Residue Study. *J. Agric. Food Chem.* **1990**, *38*, 290.

Mrozik, H.; Eskola, P.; Reynolds, G. F.; Arison, B. H.; Smith, G. M.; Fisher, M. H. Photoisomers of Avermectins. *J. Org. Chem.* **1988**, *53*, 1820.

Mrozik, H.; Eskola, P.; Linn, B. O.; Lusi, A.; Shih, T. L.; Tischler, M.; Waksmunski, F. S.; Wyvratt, M. J.; Hilton, N. J.; Anderson, T. E.; Babu, J. R.; Dybas, R. A.; Preiser, F. A.; Fisher, M. H. Discovery of Novel Avermectins with Unprecedented Insecticidal Activity. *Experimentia* **1989**, *45*, 315.

Pivnichny, J. V.; Shim, J.-S. K.; Zimmerman, L. A. Direct Determination of Avermectins in Plasma at Nanogram Levels by High-Performance Liquid Chromatography. *J. Pharm. Sci.* **1983**, *72*, 1447.

Pivnichny, J. V.; Arison, B. H.; Preiser, F. A.; Shim, J.-S. K.; Mrozik, H. Base-Catalyzed Isomerization of Avermectins. *J. Agric. Food Chem.* **1988**, *36*, 826.

Received for review November 6, 1991. Accepted January 22, 1992.